

Supporting information

α -DTC₇₁ Fullerene Performs Significantly Better than β -DTC₇₁ as Electron Transporting Material in Perovskite Solar Cells.

Edison Castro,^{a†*} Olivia Fernandez-Delgado,^{a†} Albert Artigas,^b Gerardo Zavala,^a Fang Liu,^c Antonio Moreno-Vicente,^d Antonio Rodríguez-Forteza,^d José D. Velasquez,^{a,e} Josep M. Poblet,^d and Luis Echegoyen^{a*}

^a Department of Chemistry, University of Texas at El Paso, 500 West University Avenue, El Paso, TX 79968, United States

^b Institut de Química Computacional i Catàlisi (IQCC), Department de Química, Universitat de Girona, 17003 Girona, Catalonia, Spain.

^c Department of Chemistry, Columbia University, New York, New York 10027, United States

^d Departament de Química Física i Inorgànica, Universitat Rovira i Virgili, Marcel·lí Domingo 1, 43007, Tarragona (Spain)

^e Departamento de Química, Facultad de Ciencias Naturales y Exactas, Universidad del Valle, A.A. 25360 Cali, Colombia

eacastroportillo@utep.edu

echegoyen@utep.edu

TABLE OF CONTENTS

General materials and methods	S1
Preparation of α -DTC ₇₀	S4
Preparation of β -DTC ₇₀	S5
¹ H and ¹³ C NMR spectra	S7
Compound α -DTC ₇₀	S7
Figure S1. ¹ H NMR spectrum (400 MHz, CDCl ₃).....	S7
Figure S2. ¹³ C NMR spectrum (100 MHz, CDCl ₃).....	S8
Compound 4	S9
Figure S3. ¹ H NMR spectrum (400 MHz, CDCl ₃).....	S9
Figure S4. ¹³ C NMR spectrum (100 MHz, CDCl ₃).....	S10
Compound β -DTC ₇₀	S11
Figure S5. ¹ H NMR spectrum (400 MHz, CDCl ₃ /CS ₂).....	S11
Figure S6. ¹³ C NMR spectrum (100 MHz, CDCl ₃ /CS ₂).....	S12
Figure S7. UV-Vis spectra	S13
Figure S8. Cyclic Voltammetry.....	S13
MALDI-TOF MS	S13
Figure S9. α -DTC ₇₀	S13
Figure S10. β -DTC ₇₀	S14
Figure S11. XRD characterization of the perovskite layer.....	S15
Figure S12. Power conversion efficiency distributions.....	S15
Figure S13. Electron mobility measurements.	S16
Table S1. Electron mobility values	S16
Figure S14. Electrochemical impedance spectroscopy for the fullerene-PSCs based devices. ...	S17
Table S2. Fitting parameters for EIS.....	S17
Figure S15. Schematic representation of the different beta isomers. In the case of β 1 the carbonyl near the pentagon is pointing to a lead ion whereas in β 2, the carbonyl closer to the hexagon is the one that points the lead. R are used to represent the 2-ethylthiophene fragments.	S17

Figure S16. Schematic representation of the two orientations (cap and equatorial) on the different adsorption sites (hollow, bridge and top) for the pristine C ₇₀ and their relative energies (in eV).	S18
Figure S17. Enlarged view of the shortest fullerene-Pb contacts for the lowest in energy of α-DTC ₇₀ and β-DTC ₇₀ adducts adsorbed on the MAPbI ₃ surface.	S18
References	S18

General materials and methods

All chemicals were reagent grade. Silica gel (40-60 μ , 60 \AA) was used to separate and purify the products. Matrix-assisted laser desorption/ionization time-of-flight mass spectroscopy (MALDI-TOF-MS) was conducted on positive mode, with samples dissolved in carbon disulfide and 1,1,4,4-tetraphenyl-1,3-butadiene (TPB) as matrix. NMR spectra were recorded using a Bruker 400 MHz spectrometer. The UV/Vis-NIR spectra were recorded for chloroform solutions. Cyclic voltammetry (CV) experiments were carried out under an argon atmosphere at room temperature. The scan rate for the CV experiments was 100 mV/s. A one compartment cell with a standard three-electrode set up was used, consisting of a 1 mm diameter glassy carbon disk as the working electrode, a platinum wire as the counter electrode and a silver wire as a pseudo-reference electrode, in a solution of anhydrous o-DCB containing 0.05 M n-Bu₄NPF₆. Ferrocene was added to the solution at the end of each experiment as an internal standard.

Device Fabrication

PC₇₁BM was bought from SES Research. Methylammonium iodide (CH₃NH₃I, 99.5%) was bought from Greatcellsolar. PbI₂ (99%) was bought from Sigma-Aldrich. The configuration used for the fabrication of the PSCs was ITO/PEDOT:PSS/CH₃NH₃PbI₃/ETM/Ag. The patterned ITO glass substrates were cleaned sequentially with detergent, deionized water and acetone, each step for 30 min, then dried with nitrogen gas and finally treated in a UV-ozone oven for 30 min. After passing through a 0.45 μ m PVDF filter, the PEDOT:PSS solution (Baytron P VP AI 4083) was spin-coated onto the treated ITO substrates at 5000 rpm for 30 s and heated at 150 °C for 15 min in air. Then the substrates were transferred to a N₂-filled glovebox where CH₃NH₃PbI₃ (1 M solution in DMF) was spin-coated on top of the PEDOT:PSS coated substrates at 800 rpm for 10 s and at 4000 rpm for 25 s. 80 μ L of toluene were added 5 s after the second step and then the devices were annealed at 70 °C for 60 min (a pure perovskite film without apparent pinholes was observed by XRD characterization). The fullerene derivatives dissolved in chlorobenzene (20 mg/mL) were spin-coated onto the CH₃NH₃PbI₃ layer at 5000 rpm for 30 s. Finally, Ag electrodes (100 nm) were deposited by thermal evaporation under a pressure of 1×10^{-6} Torr through a shadow mask. The active area of the fabricated devices was 6 mm². The Ag electrodes were encapsulated with a UV-curable epoxy resin and a glass slide before testing. Stability studies were conducted on unencapsulated devices under 50% humidity at ambient conditions for 7 days. All devices were tested using a 6 mm² mask to avoid light scattering. The electron mobility (μ_e) values of all fullerenes-based devices were measured using the space charge limit current (SCLC) method,¹ and using the dark J - V curves of electron-only devices with the configuration of ITO/Al/ETM/Al.

Device Characterization

Current-Voltage (J - V) characteristics of photovoltaic cells were tested using a Keithley 2420 source meter under a Photo Emission Tech SS100 Solar Simulator, and the light intensity was calibrated by a standard Si solar cell. External quantum efficiency (EQE) was measured using a Bentham (from Bentham Instruments Ltd) measurement system. The light intensity was calibrated using a single-crystal Si photovoltaic cell as reference. The J - V and EQE measurements were obtained in air. The scanning electron microscopy (SEM) images were collected using a ZEISS Sigma FE-SEM, where the electron beam was accelerated in the range of 500 V to 30 kV. Film thicknesses were measured using a KLA Tencor profilometer.

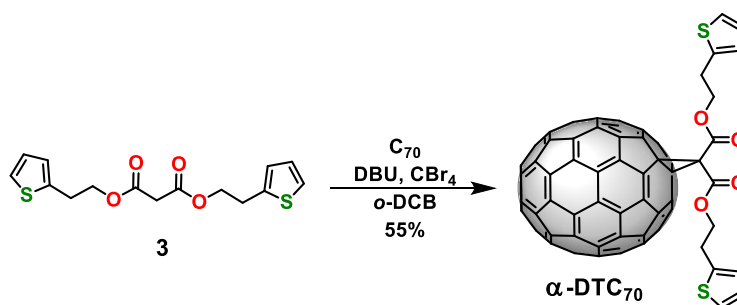
The steady photoluminescence (PL) spectra were collected with a home-built inverted microscope setup (Nikon, Eclipse TE300 inverted microscope), using 2.75 eV excitation from a diode laser (CNI laser, MDL-III-450-1W). The excitation laser passed through an ND 3.0 filter and reflected by a 490 nm long pass dichroic mirror and passed through a 50X objective to focus at the sample surface. The emission collected from the same objective and dichroic mirror was focused into a spectrograph (SPEX 270M) with 300l/mm grating and detected by a liquid-N₂ cooled CCD array detector (RS Roper Scientific CCD-512-TKB).

The time-dependent decay of PL signal was measured using MicroTime 200 time-resolved fluorescence microscope (PicoQuant), equipped with an inverted microscope setup (Olympus, IX73 inverted microscope) and a 405 nm excitation laser (MicroTime LDH-D-C-405). All optical measurements of the sample were carried out in a N₂ gas filled cell at room temperature.

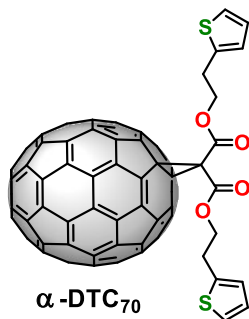
DFT calculations

All calculations were performed using DFT method with a generalized gradient approximation (GGA) and Perdew-Burke-Ernzerhof (PBE) exchange-correlation functional as implemented in the all-electron code Fritz Haber Institute ab initio molecular simulations (FHI-aims).² The van der Waals interactions were corrected via Tkatchenko and Scheffler corrections (DFT-TS). We have used a two-layer 2 x 2 supercell of the CH₃NH₃PbI₃ (110) surface with a vacuum thickness set to 19 Å. The CH₃NH₃I atoms in the bottom layer were fixed at the bulk positions while other atoms were relaxed. The convergence threshold for the self-consistent iteration was set to 10⁻⁵ eV, and the non-fixed atomic positions were fully optimized until the force on each atom was less than 0.005 eV/Å. The adsorption energies (E_{ads} , eV) for X-DTC₇₀-CH₃NH₃PbI₃ were calculated using $E_{\text{ads}} = E(\text{X-DTC}_{70}\text{-CH}_3\text{NH}_3\text{PbI}_3) - E(\text{CH}_3\text{NH}_3\text{PbI}_3) - E(\text{DTC}_{70})$, X-DTC₇₀ = α -DTC₇₀, β -DTC₇₀, where $E(\text{structure})$ is the calculated energy of the corresponding structure.

Preparation of α -DTC₇₀

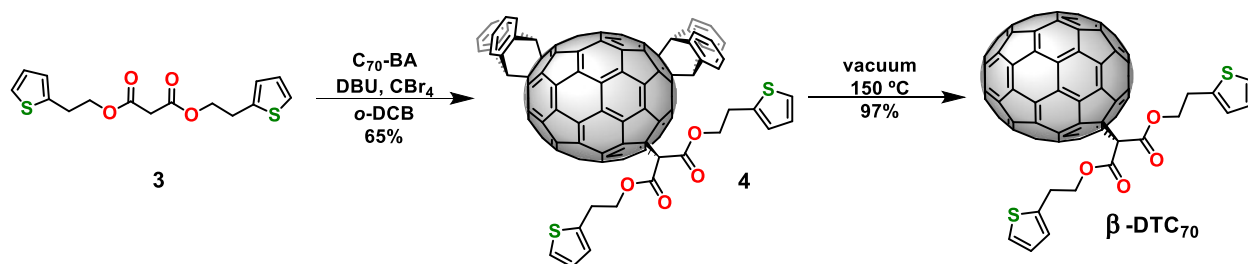


In a two-necked round-bottom flask equipped with a magnetic stirrer, an inert atmosphere and protected from light, a mixture of C_{70} (84 mg, 0.10 mmol, 1 equiv.), CBr_4 (66 mg, 0.20 mmol, 2 equiv.) and malonate derivative **3** (32 mg, 0.10 mmol, 1 equiv.) was prepared in anhydrous o-DCB (10 mL). 8-Diazabicyclo[5.4.0]undec-7-ene (DBU) (30 μL , 30 mg, 0.2 mmol, 2 equiv.) was added and the reaction mixture was left stirring for 0.5 h at room temperature. The reaction mixture was directly subjected to purification by column chromatography (SiO_2 , 40–63 μm , $\text{CS}_2 \rightarrow \text{CS}_2/\text{CHCl}_3$ 10:1) to provide α -DTC₇₀ (64 mg, 0.055 mmol, 55% overall yield) as a black solid. The analytical samples were prepared by washing α -DTC₇₀ with MeOH (2 x 3 mL) and pentane (2 x 3 mL).

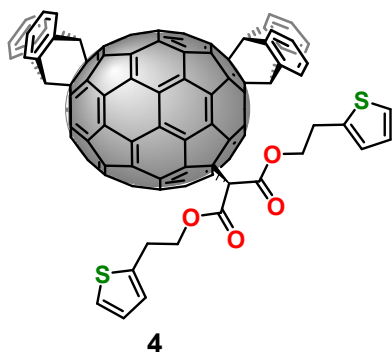


¹H NMR (400 MHz, $\text{CDCl}_3/\text{CS}_2$) δ (ppm): 7.18 (t, $J = 3.5$ Hz, 1H), 6.95 (d, $J = 3.5$ Hz, 2H), 4.62 (t, $J = 6.6$ Hz, 2H), 3.31 (t, $J = 6.6$ Hz, 2H); **¹³C NMR (101 MHz, $\text{CDCl}_3/\text{CS}_2$) δ (ppm):** δ 29.27, 31.09, 37.00, 66.26, 66.86, 67.44, 124.57, 126.11, 127.33, 130.93, 131.00, 131.04, 132.91, 133.66, 136.91, 139.20, 140.87, 141.77, 142.31, 142.83, 142.96, 143.66, 143.95, 144.07, 144.97, 146.01, 146.05, 146.58, 147.11, 147.42, 147.63, 147.75, 148.59, 148.63, 148.81, 149.21, 149.37, 149.45, 150.69, 150.83, 151.28, 151.44, 151.47, 155.16, 163.32; (45/45 signals detected); **UV-vis (CHCl_3) λ_{max} (nm):** 353, 369, 401, 461; **MALDI-TOF HRMS (m/z)** calc for $[\text{M}^-] = 1162.064$; found: 1162.061.

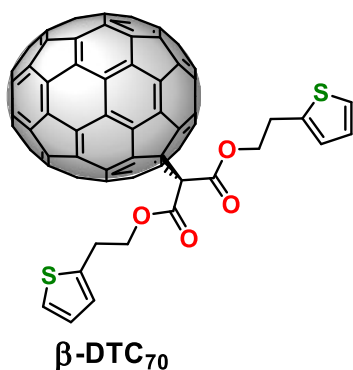
Preparation of β -DTC₇₀



In a two-necked round-bottom flask equipped with a magnetic stirrer, an inert atmosphere and protected from light, a mixture of BA-C₇₀ (35 mg, 0.029 mmol, 1,1 equiv.), CBr₄ (18 mg, 0.054 mmol, 2 equiv.) and malonate derivative **3** (8.6 mg, 0.027 mmol, 1 equiv.) was prepared in anhydrous o-DCB (15 mL). 8-Diazabicyclo[5.4.0]undec-7-ene (DBU) (8 μ L, 8.1 mg, 0.054 mmol, 2 equiv.) was added and the reaction mixture was left stirring for 16 h at room temperature. The reaction mixture was directly subjected to purification by column chromatography (SiO₂, 40–63 μ m, CS₂→CS₂/CHCl₃ 10:1). The fraction containing tris(adduct) **4** (24 mg, 0.016 mmol) was collected and concentrated under reduced pressure. The resulting black solid was heated at 150 °C under vacuum for 1 h, dissolved in CS₂ (3 mL) and purified by column chromatography (SiO₂, 40–63 μ m, CS₂/CHCl₃ 10:2) to provide β -DTC₇₀ (18 mg, 0.015 mmol, 58% overall yield) as a black solid. The analytical samples were prepared by washing β -DTC₇₀ with MeOH (2 x 3 mL) and pentane (2 x 3 mL).



¹H NMR (400 MHz, CDCl₃) δ (ppm): 7.72 (d, J = 7.8 Hz, 2H), 7.61 (d, J = 6.5 Hz, 2H), 7.57 (d, J = 7.8 Hz, 2H), 7.54 (d, J = 6.5 Hz, 2H), 7.42–7.30 (m, 8H), 7.20 (dd, J = 5.1 Hz, 1.3 Hz, 1H), 7.08 (dd, J = 5.1 Hz, 1.3 Hz, 1H), 6.96–7.00 (m, 2H), 6.84 (dd, J = 5.1 Hz, 3.4 Hz, 1H), 6.73 (dd, J = 3.4 Hz, 1.3 Hz, 1H), 5.58 (s, 1H), 5.36 (s, 1H), 5.27 (s, 1H), 5.25 (s, 1H), 4.64 (t, J = 6.6 Hz, 2H), 4.35 (t, J = 6.6 Hz, 2H), 3.32 (t, J = 6.6 Hz, 2H), 3.04 (t, J = 6.6 Hz, 2H); **¹³C NMR (101 MHz, CDCl₃) δ (ppm):** 164.2, 164.0, 159.5, 159.1, 155.9, 155.5, 153.3, 153.1, 152.6, 152.2, 151.9, 151.1, 150.8, 150.3, 150.0, 148.8, 148.7, 143.7, 143.2, 141.7, 141.5, 141.4, 141.3, 141.2, 141.1, 141.0, 140.9, 140.3, 139.7, 139.2, 139.2, 138.7, 137.9, 136.6, 136.4, 133.8, 132.7, 129.1, 128.5, 128.3, 128.3,



127.2, 127.2, 127.0, 126.0, 125.9, 125.8, 125.7, 125.6, 125.5, 125.4, 124.4, 124.9, 67.3, 66.8, 66.4, 65.8, 65.7, 65.7, 63.7, 62.3, 59.6, 58.5, 57.5, 55.9, 40.9, 29.3, 29.0 (68/68 signals detected); **UV-vis (CHCl₃) λ_{max} (nm):** 385, 459, 652.

¹H NMR (400 MHz, CDCl₃/CS₂) δ (ppm):) δ 7.24 (dd, *J* = 5.1, 1.3 Hz, 1H), 7.10 (dd, *J* = 5.1, 1.3 Hz, 1H), 7.03 – 6.97 (m, 2H), 6.86 (dd, *J* = 5.1, 3.4 Hz, 1H), 6.74 (dd, *J* = 3.4, 1.3 Hz, 1H), 4.67 (t, *J* = 6.6 Hz, 2H), 4.31 (t, *J* = 6.6 Hz, 2H), 3.35 (t, *J* = 6.6 Hz, 2H), 3.05 (t, *J* = 6.6 Hz, 2H); **¹³C NMR (101 MHz, CDCl₃/CS₂) δ (ppm):** 163.4, 162.9, 153.0, 151.4, 149.8, 149.5, 149.5, 149.4, 149.1, 148.8, 148.6, 148.6, 148.2, 148.2, 147.5, 147.4, 147.1, 147.0, 147.0, 146.5, 146.0, 145.3, 145.1, 145.0, 144.9, 144.6, 144.4, 143.5, 143.4, 141.4, 139.5, 139.1, 138.9, 138.2, 132.0, 131.8, 131.3, 127.8, 127.2, 127.0, 126.0, 125.7, 124.5, 124.3, 77.1, 67.3, 66.9, 61.3, 38.2, 29.2, 28.9 (50/52 signals detected); **UV-vis (CHCl₃) λ_{max} (nm):** 371, 440; **MALDI-TOF HRMS: MALDI-TOF HRMS (*m/z*)** calcd for [M⁻] = 1162.064; found: 1162.066.

^1H and ^{13}C NMR spectra

Compound $\alpha\text{-DTC}_{70}$

Figure S1. ^1H NMR spectrum (400 MHz, CDCl_3)

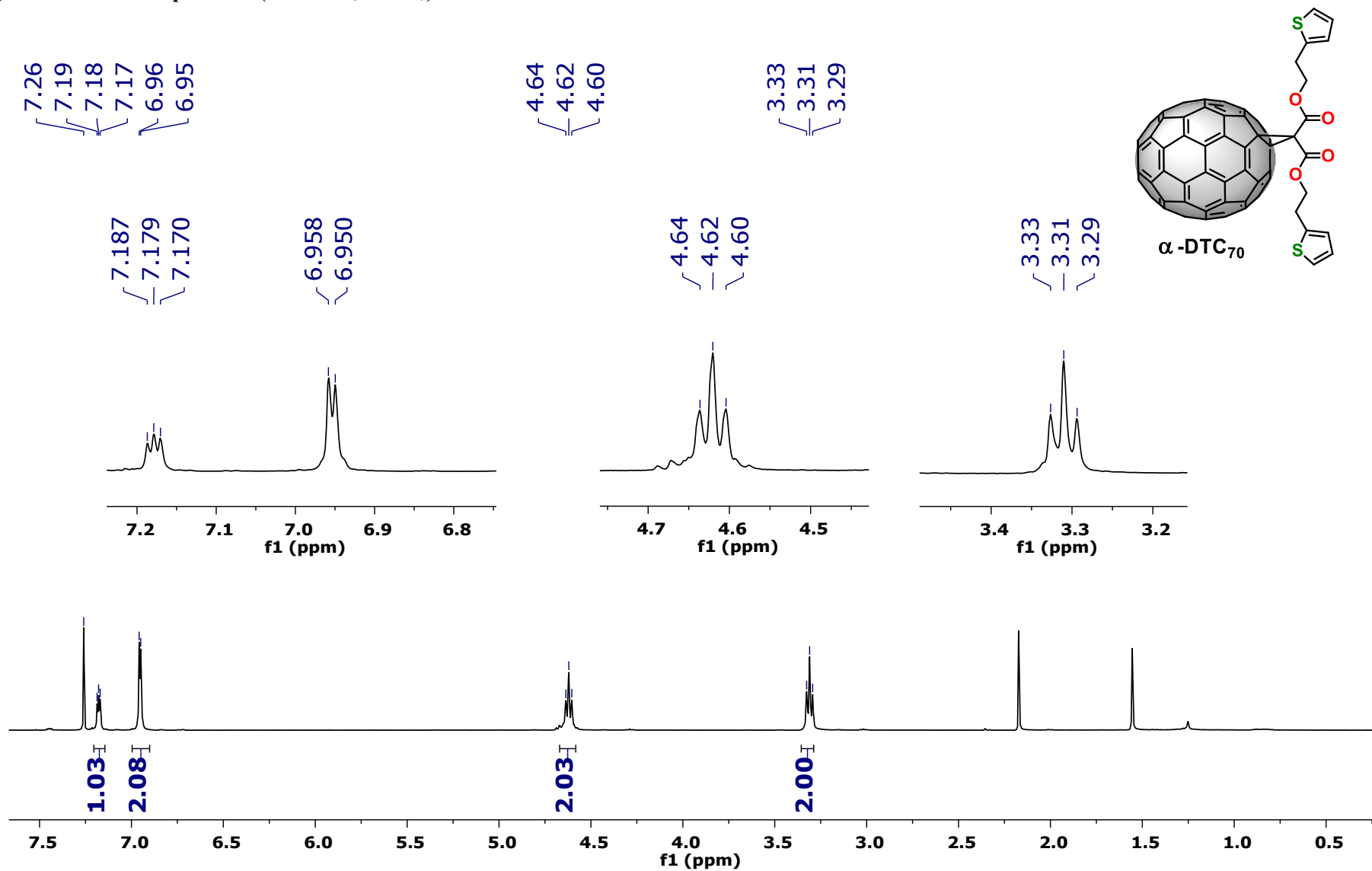
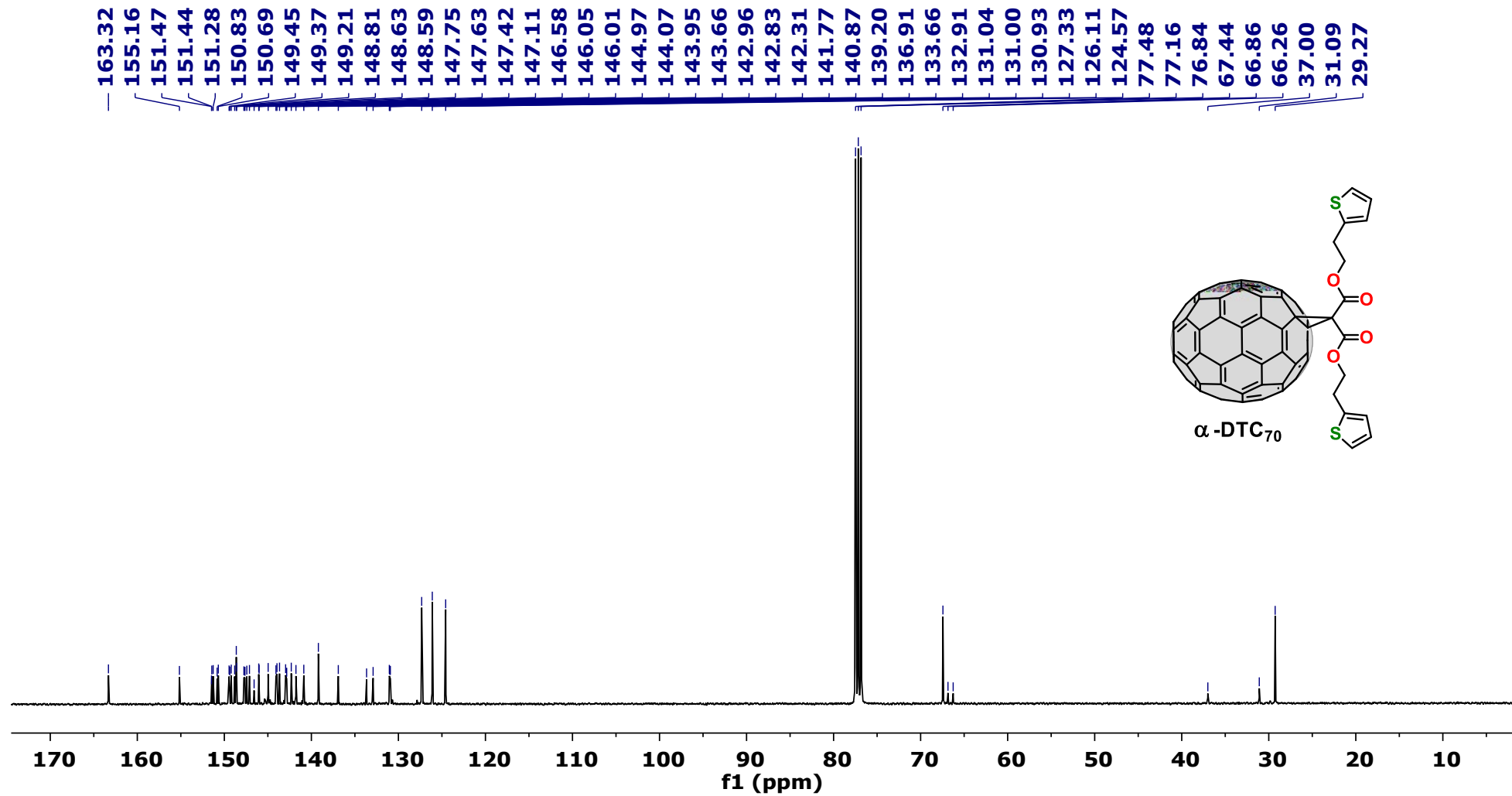


Figure S2. ¹³C NMR spectrum (100 MHz, CDCl₃)



Compound 4

Figure S3. ¹H NMR spectrum (400 MHz, CDCl₃)

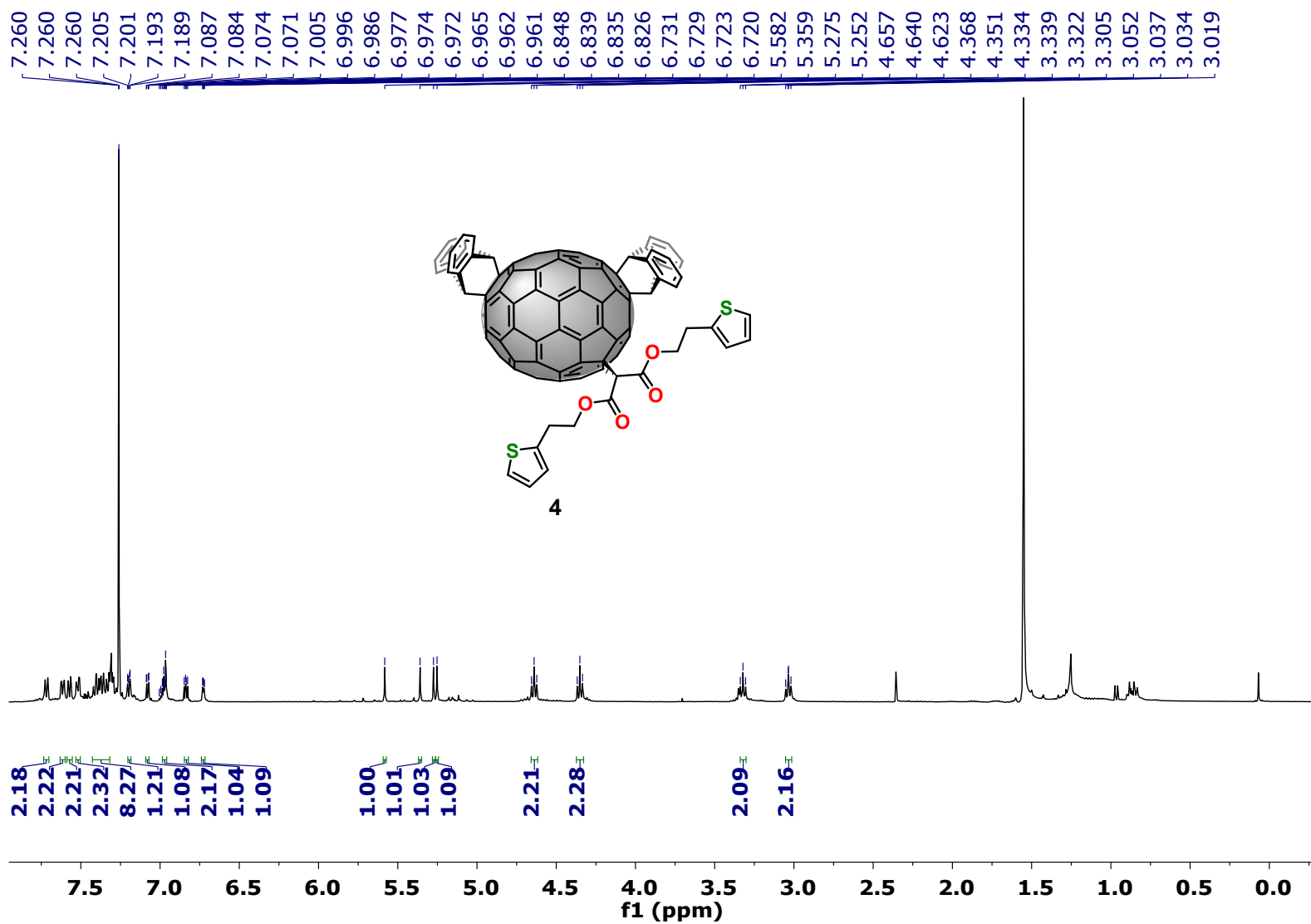
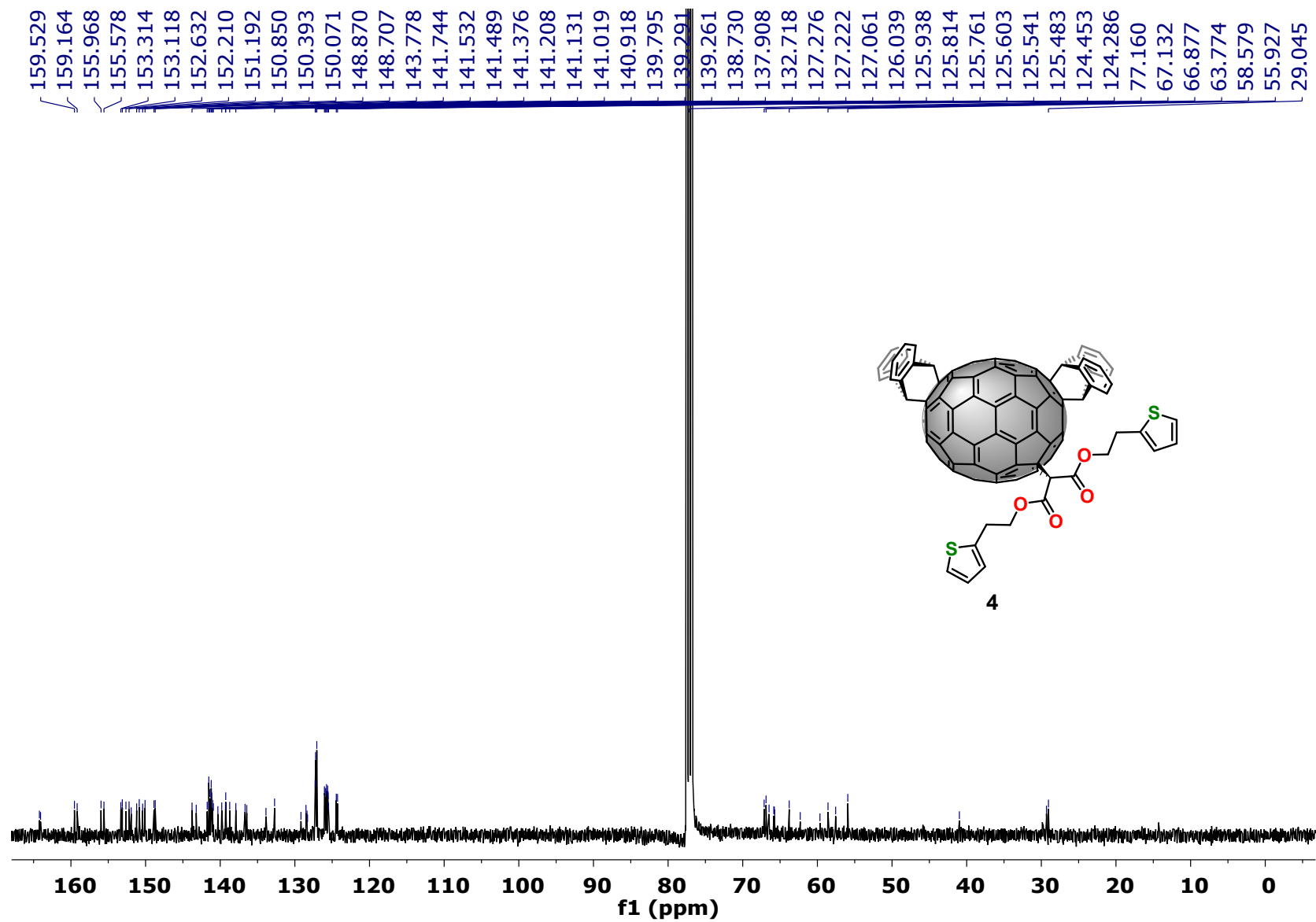


Figure S4. ^{13}C NMR spectrum (100 MHz, CDCl_3)



Compound β -DTC₇₀

Figure S5. ¹H NMR spectrum (400 MHz, CDCl₃/CS₂)

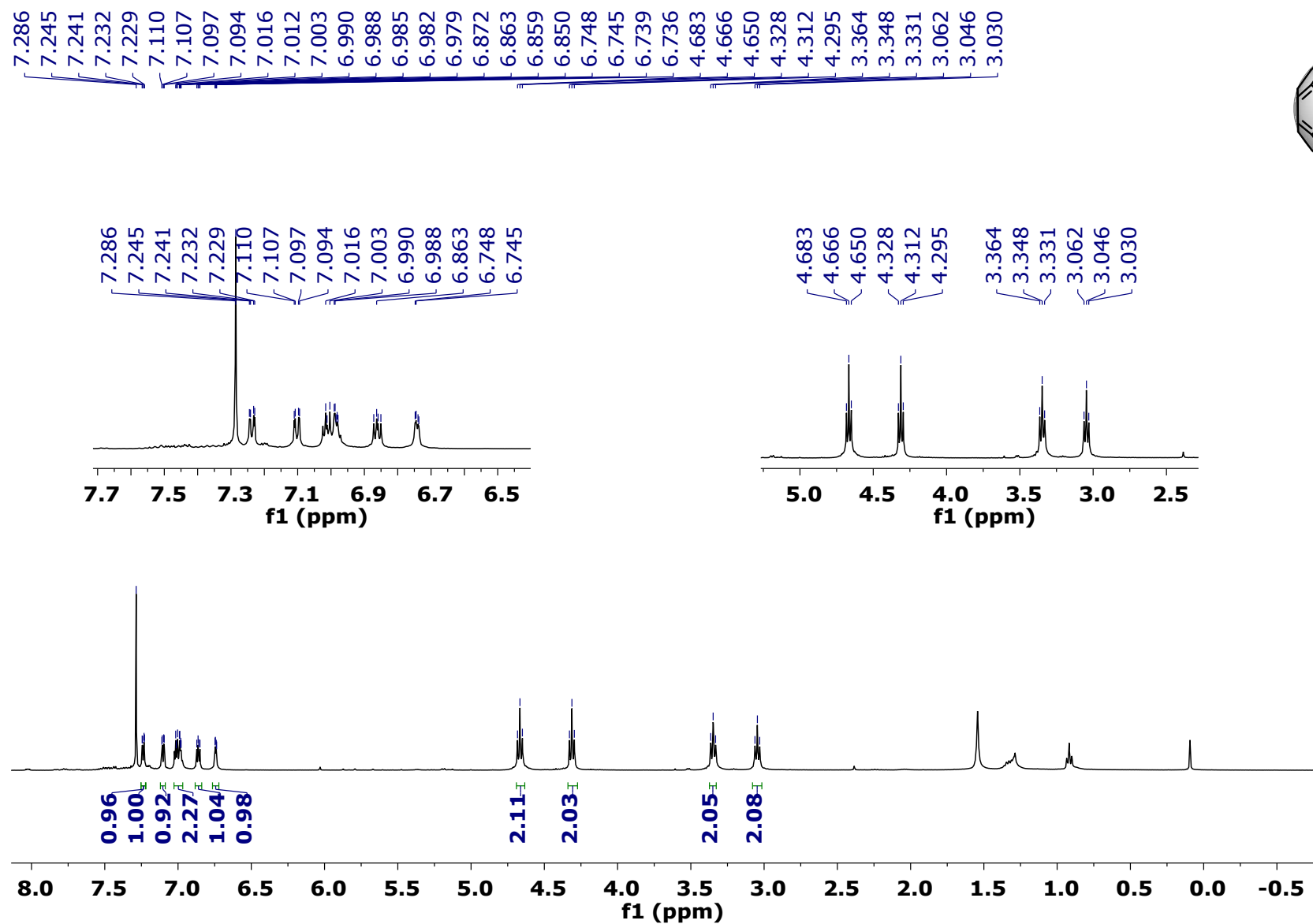


Figure S6. ^{13}C NMR spectrum (100 MHz, $\text{CDCl}_3/\text{CS}_2$)

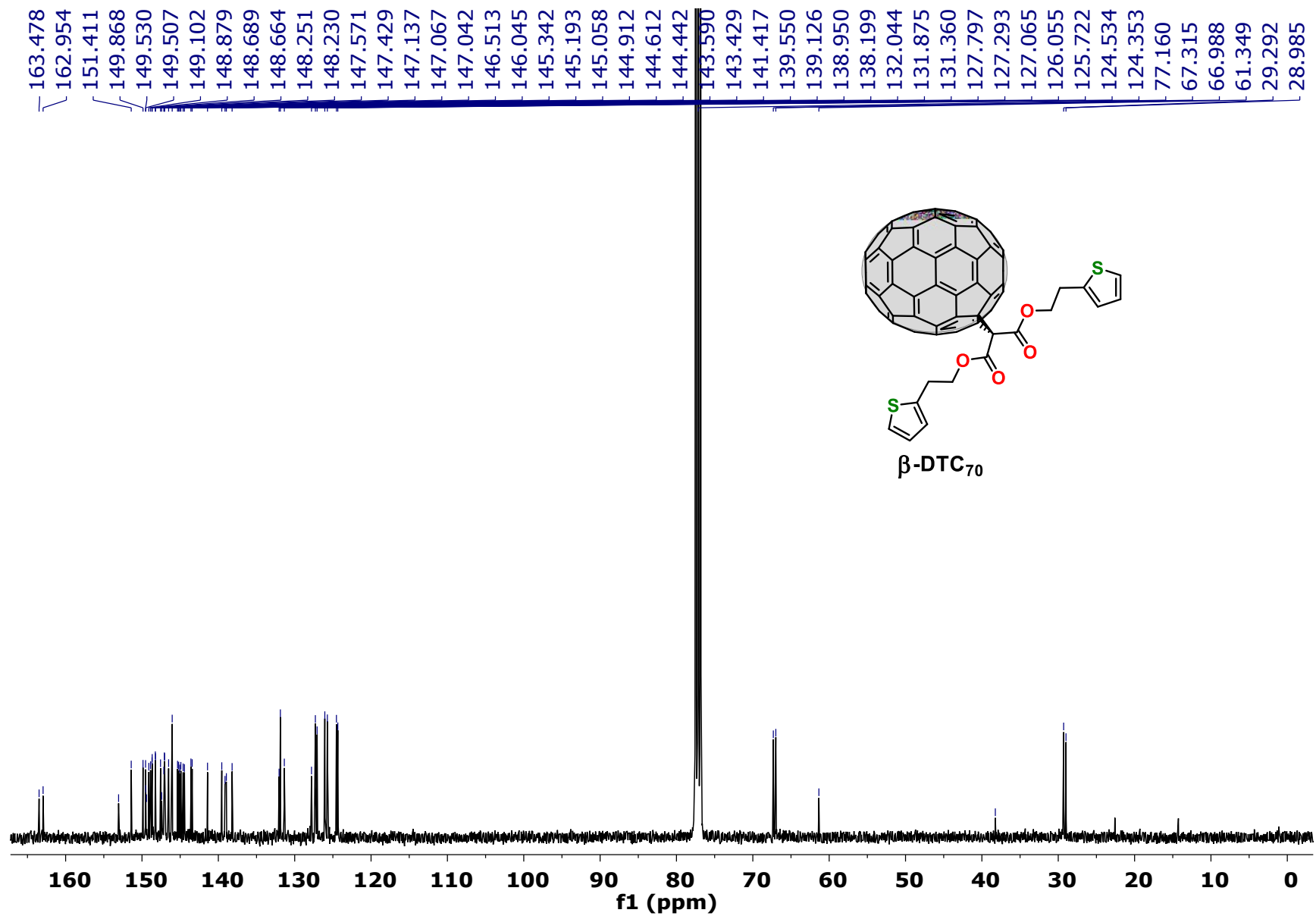


Figure S7. UV-Vis spectra

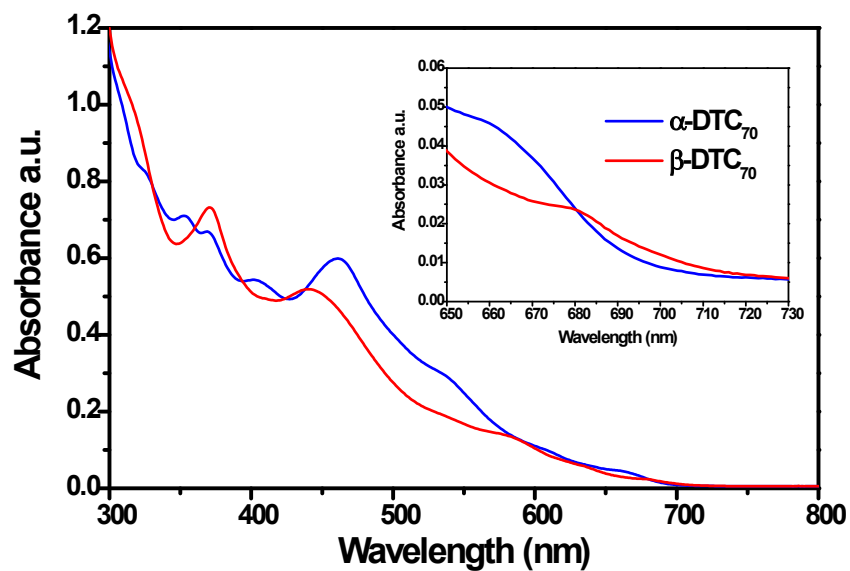
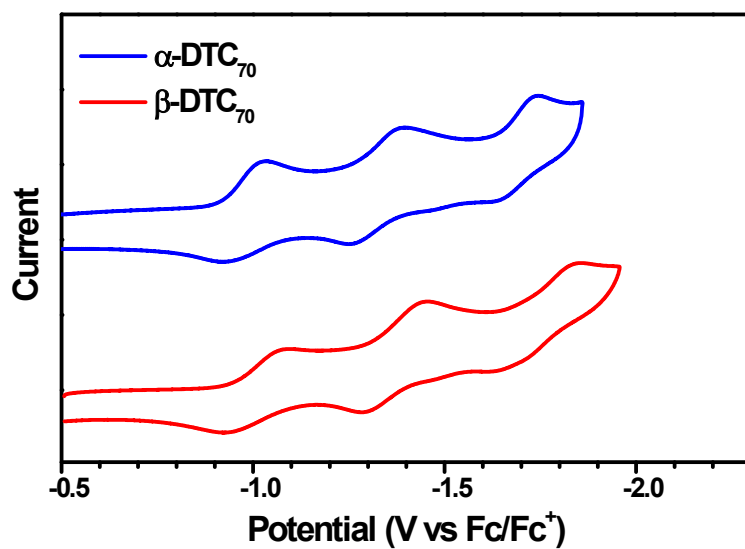


Figure S8. Cyclic Voltammetry



MALDI-TOF MS

Figure S9. α -DTC₇₀

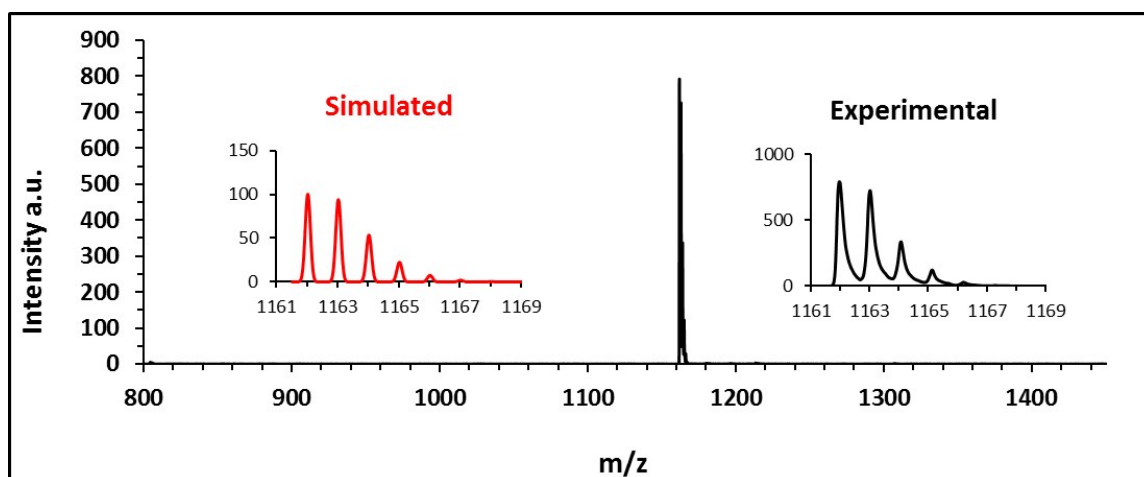


Figure S10. β -DTC₇₀

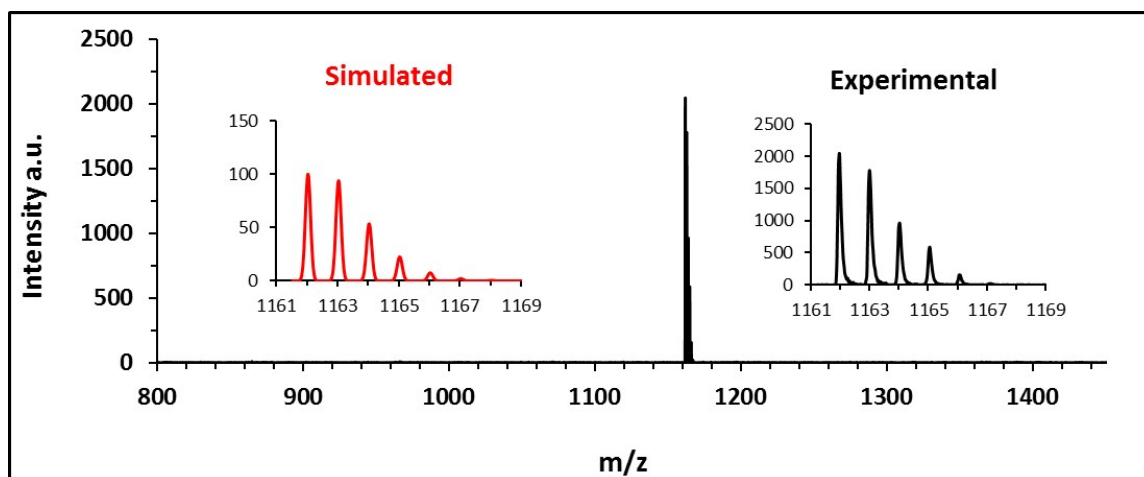


Figure S11. XRD characterization of the perovskite layer

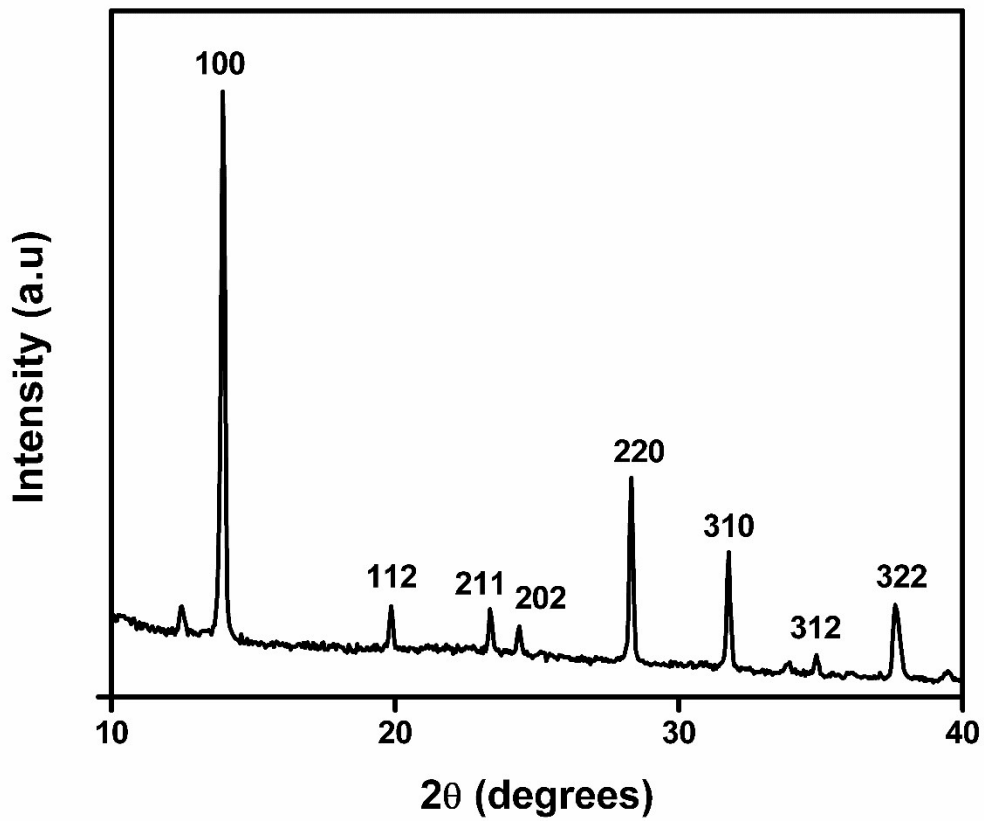


Figure S12. Power conversion efficiency distributions

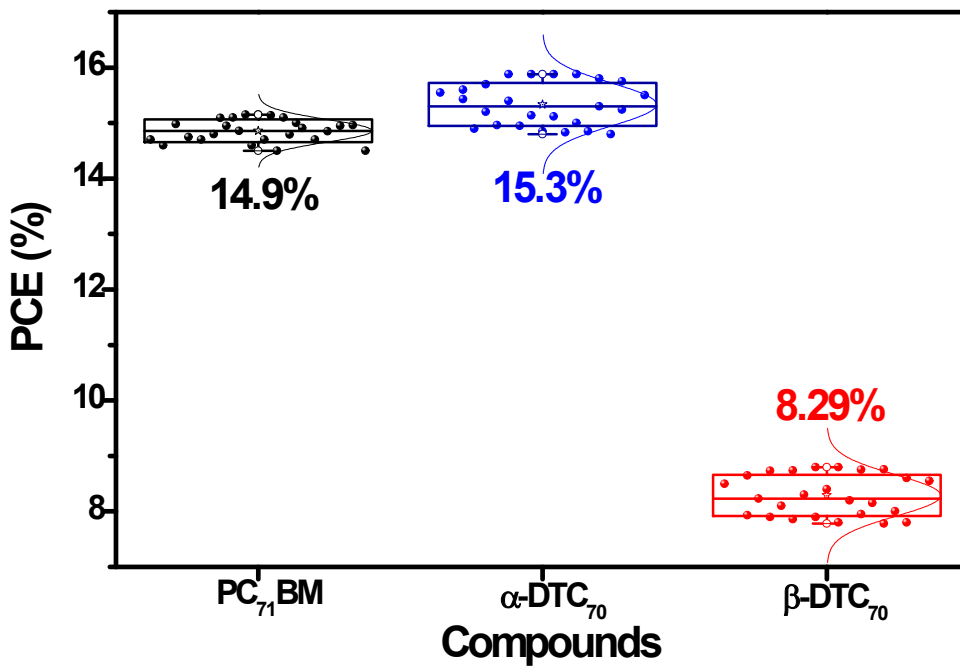


Figure S13. Electron mobility measurements.

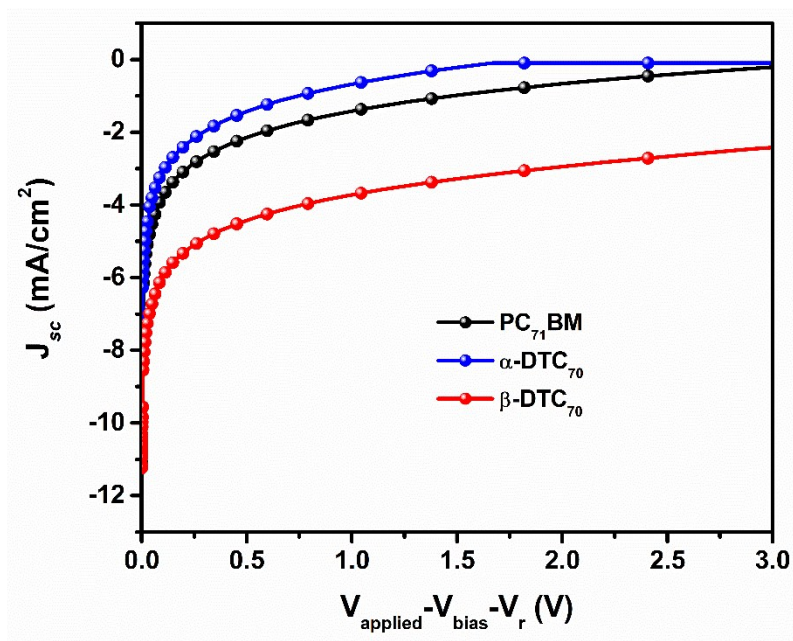


Table S1. Electron mobility values

Compound	Electron mobility ($\text{cm}^2\text{V}^{-1}\text{s}^{-1}$)	Standard deviation	Standard error
PC ₇₁ BM	$3.63 \cdot 10^{-3}$	$6.29 \cdot 10^{-6}$	$3.64 \cdot 10^{-6}$
α -DTC ₇₀	$3.68 \cdot 10^{-3}$	$2.92 \cdot 10^{-6}$	$1.69 \cdot 10^{-6}$
β -DTC ₇₀	$3.51 \cdot 10^{-3}$	$7.72 \cdot 10^{-6}$	$4.45 \cdot 10^{-6}$

Figure S14. Electrochemical impedance spectroscopy for the fullerene-PSCs based devices.

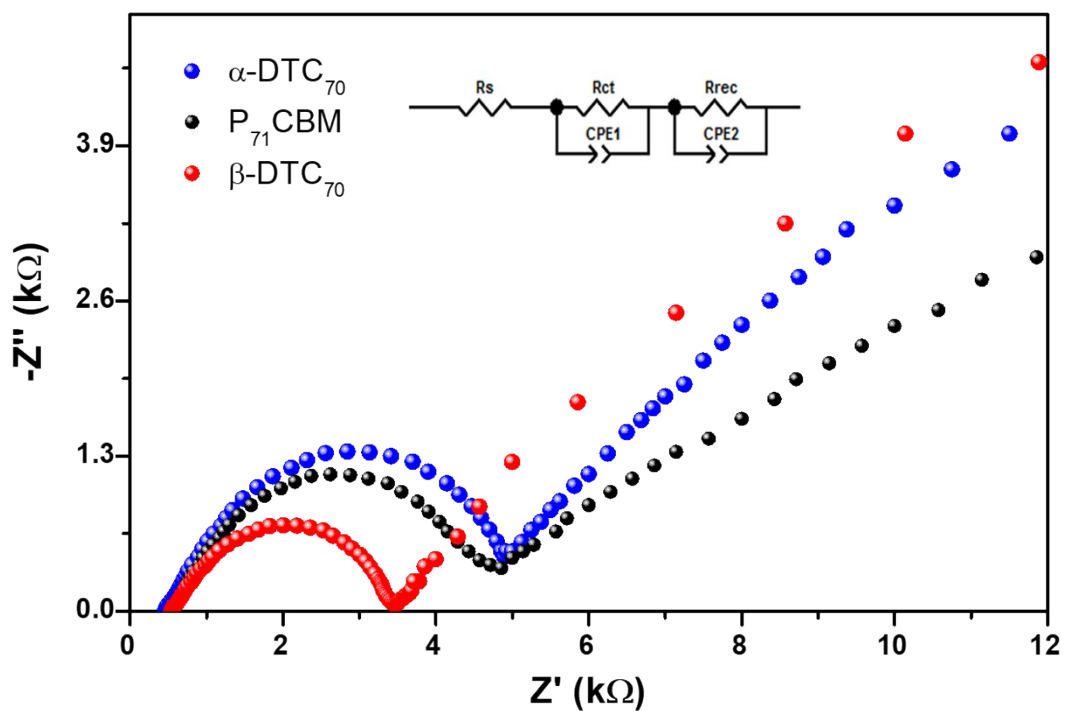


Table S2. Fitting parameters for EIS.

Device	R_s (k Ω)	R_{rec} (k Ω)	R_{ct} (k Ω)
α -DTC ₇₀	1.23	4.51	24.43
PC ₇₁ BM	1.35	4.25	32.18
β -DTC ₇₀	1.69	2.89	29.68

Figure S15. Schematic representation of the different beta isomers. In the case of $\beta 1$ the carbonyl near the pentagon is pointing to a lead ion whereas in $\beta 2$, the carbonyl closer to the hexagon is the one that points the lead. R are used to represent the 2-ethylthiophene fragments.

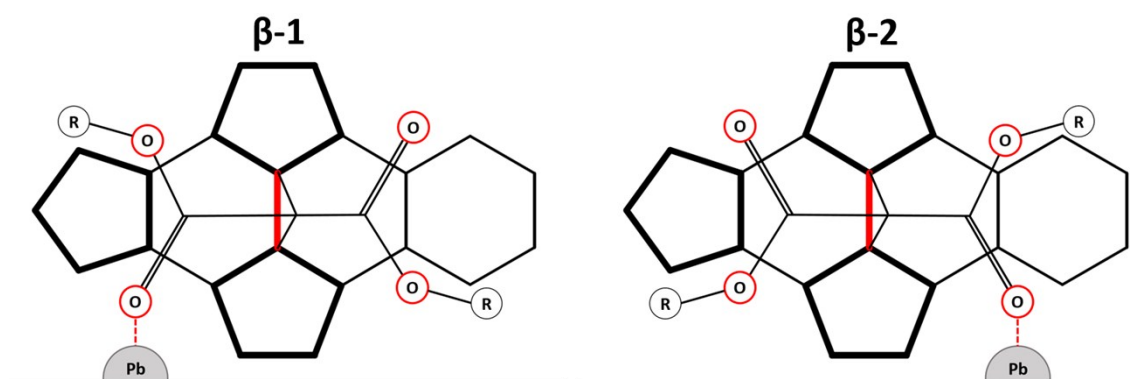


Figure S16. Schematic representation of the two orientations (cap and equatorial) on the different adsorption sites (hollow, bridge and top) for the pristine C_{70} and their relative energies (in eV). The red arrow refers to the C_5 axis. For example, labels HC and BE represent hollow-cap and bridge-equatorial, respectively. The adsorption energy for the HC site is -1.81 eV

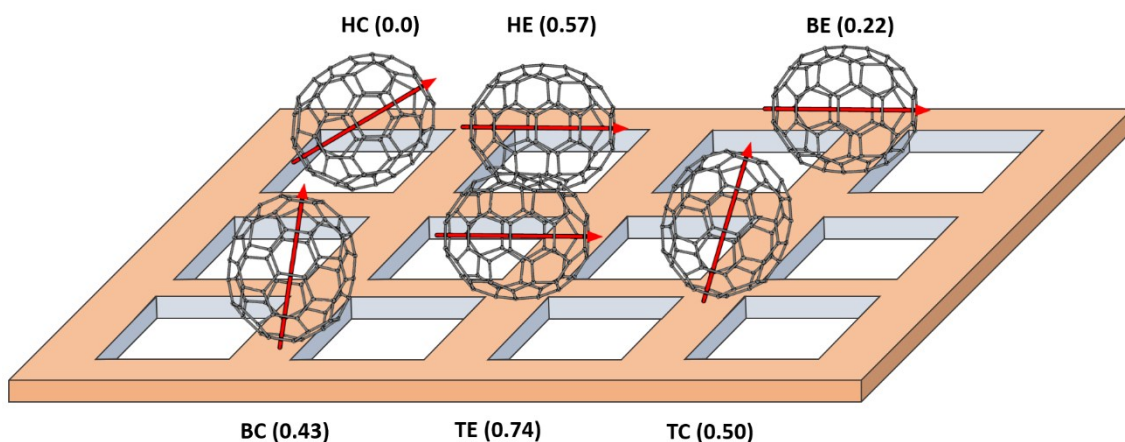
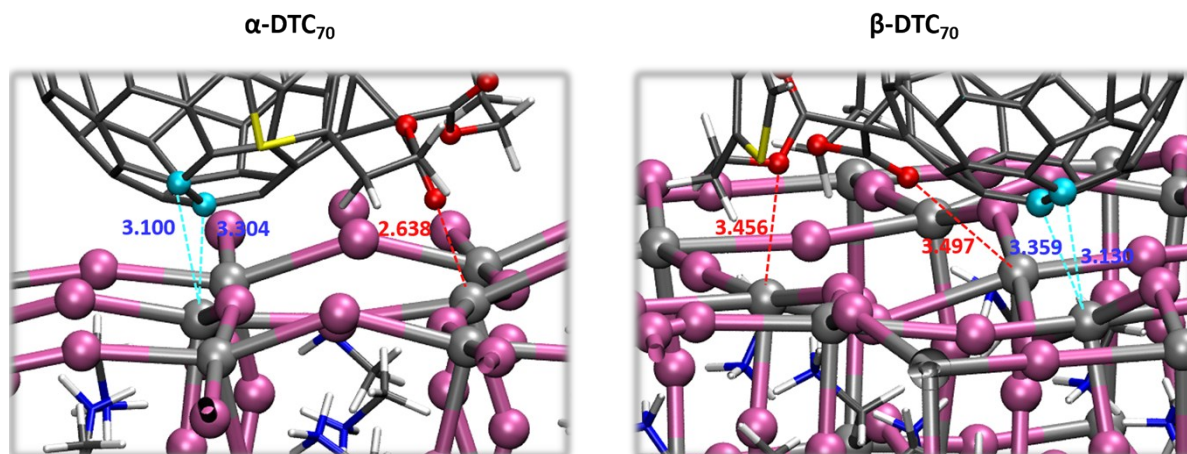


Figure S17. Enlarged view of the shortest fullerene-Pb contacts for the lowest in energy of α -DTC $_{70}$ and β -DTC $_{70}$ adducts adsorbed on the MAPbI $_3$ surface. Carbon atoms of the fullerene closer to Pb atoms are represented in cyan.



References

1. P. N. Murgatroyd, *J. Phys. D: Appl. Phys.*, 1970, **3**, 151.
2. V. Blum, R. Gehrke, F. Hanke, P. Havu, V. Havu, X. Ren, K. Reuter and M. Scheffler, *Computer Physics Communications*, 2009, **180**, 2175-2196.